



## Embryonic staging of the brown garden snail, *Cornu aspersum* (Gastropoda: Stylommatophora), an emerging model gastropod

Kaitlyn M. Abshire<sup>1,2</sup> and Prashant P. Sharma<sup>1,2</sup>

<sup>1</sup>*Department of Integrative Biology, University of Wisconsin-Madison, Madison, WI 53706, USA; and*  
<sup>2</sup>*Zoological Museum, University of Wisconsin-Madison, Madison, WI 53706, USA*

Correspondence: K. M. Abshire; e-mail: [kmabshire@wisc.edu](mailto:kmabshire@wisc.edu)

(Received 27 November 2024; editorial decision 13 April 2025)

### ABSTRACT

Comparative developmental research within Gastropoda has flourished in recent decades with modern advancements in imaging techniques and experimental manipulations. Data from marine and aquatic gastropod models have proven vital to understanding morphogenetic processes such as spiral cleavage and the establishment of chirality. However, there remains a paucity of knowledge on terrestrial pulmonate gastropod embryonic development, which impedes investigating major evolutionary transitions within Gastropoda, with emphasis on terrestrialization. The brown garden snail *Cornu aspersum* (Stylommatophora: Helicidae) is an economically, medically and environmentally important pulmonate gastropod with a widespread distribution. Here, we provide a description of the complete embryonic development of *C. aspersum* and an embryonic staging system in tandem with protocols for *in ovo* culture, immunohistochemistry and fluorescent *in situ* hybridization.

### INTRODUCTION

Gastropoda is the most diverse class of the phylum Mollusca, with over 100,000 described extant species comprising *c.* 80% of all known molluscs (Bieler, 1992; Brown & Lydeard, 2010; Haszprunar & Wanninger, 2012). Among gastropods, snails and slugs are one of the few metazoan taxa that can thrive in myriad environments, successfully inhabiting terrestrial, freshwater and marine habitats (Bieler, 1992; Brown & Lydeard, 2010). Their success and widespread distribution can be largely attributed to their diverse morphology, ecology and trophic specialization across lineages (Yang *et al.*, 2020). Understanding how distinctive gastropod lineages diversified and colonized terrestrial habitats commands significant biological interest, yet only a few gastropod species have been studied within the context of evolutionary developmental biology, and even fewer terrestrial exemplars.

Gastropod models for comparative developmental research emerged towards the end of the 19th century (Lesoway & Henry, 2019). Spiral-cleaving embryos of *Crepidula fornicata* (slipper snail) and *Ilyanassa obsoleta* (mud snail) were used to explore early embryonic development and patterns of spiral cleavage (Clement, 1962; Conklin, 1897). Recent advances in imaging techniques and experimental manipulations have propelled the utility of gastropod models for understanding morphogenetic processes, such as cell fate specification, left-right asymmetry, and gastrulation (Grande & Patel, 2009; Kuroda & Abe, 2020; Lyons *et al.*, 2012, 2015). Additionally, the increasing availability of high-throughput sequence data and emerging utilization of functional genetic tech-

niques (e.g. RNAi, CRISPR/Cas9) have allowed researchers unprecedented opportunities to establish new gastropod models for evo-devo (e.g. *Lymnaea stagnalis*, *Biomphalaria glabrata*, *Berghia stephanieae* and *Pomacea canaliculata*) and provide deep insights into complex biological processes, such as biomineralization, torsion and chemosensory reception (Knight *et al.*, 2011; Perry & Henry, 2014; Kuroda & Abe, 2020; Acorsi *et al.*, 2024; Goodheart *et al.*, 2024).

Despite these advances, the absence of terrestrial gastropod models for the study of comparative development represents a hurdle for investigating major evolutionary transitions, with emphasis on terrestrialization, shell reduction and loss (= limacization), untwisting of the neural visceral loop (= orthoneury), and the specification of head tentacles (Barker, 2001; Ruthensteiner, 1997; Brenzinger *et al.*, 2021). To address this gap, the brown garden snail, *Cornu aspersum* (Eupulmonata: Stylommatophora: Helicidae), is well poised to serve as a terrestrial model for comparative study (Fig. 1A, B). Stylommatophora is the second-largest order of Gastropoda, with over 25,000 described species (Barker, 2001; Rosenberg, 2014). Distinguishing them from other gastropod groups, stylommatophorans have a combination of unique features, such as a vascularized pallial lung cavity; a contractile pneumostome; two distinct pairs of cylindrical, retractile head appendages; a secondary ureter; a long tongue-shaped suprapedal gland on the floor of their visceral body; and simultaneous hermaphroditism (Burch, 1962; Barker, 2001; Dayrat & Tillier, 2002; Mordan & Wade, 2008). Within Stylommatophora, *Cornu aspersum* is one of the most widespread terrestrial

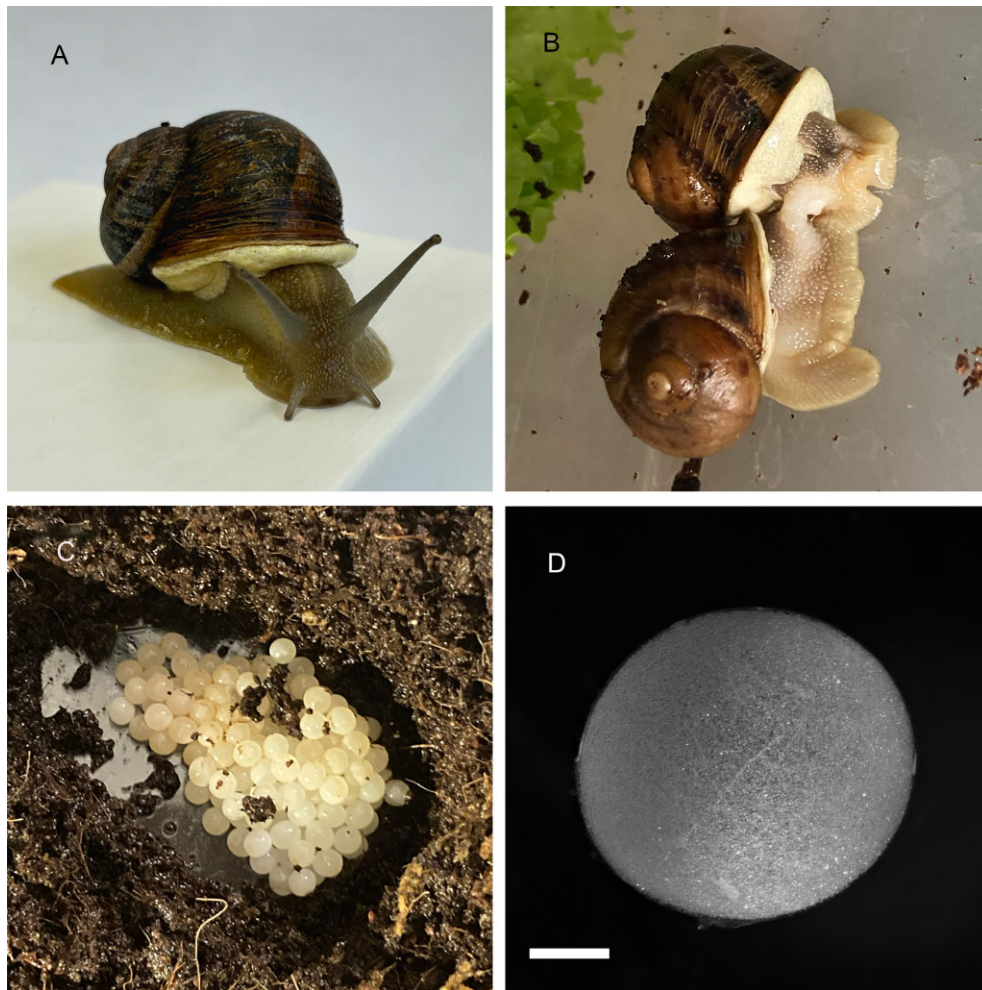


**Figure 1.** *Cornu aspersum*. **A.** Adult in anterior view. **B.** A mating pair. **C.** Egg clutch, uncovered from substrate. **D.** Detail of a single egg. Scale bar: 500  $\mu\text{m}$ .

air-breathing snails and is abundant in many rural and urban habitats that have a Mediterranean, temperate or subtropical climate (Guiller & Madec, 2010). With rapid onset of sexual maturity within ca. 6 months and a high reproductive capacity of multiple clutches of eggs (100–200 eggs per clutch) (Fig. 1C, D), *C. aspersum* has been used intensively in snail farming for culinary, cosmetic and medical purposes (Madec *et al.*, 2000; Smith, 2010; McDermott *et al.*, 2021). Furthermore, *C. aspersum* has been used as an environmental index species for soil and air quality in urban and industrial areas (Itziou *et al.*, 2018; Georgescu *et al.*, 2021). The economic, medical and environmental significance of *C. aspersum* readily positions this species as a useful model for broader biological studies.

A previous work on *C. aspersum* documented the architecture of its neural system, suggesting a promising model for laboratory studies of Stylommatophora (Ierusalimsky & Balaban, 2001). Other studies on *C. aspersum* embryogenesis have either focused exclusively on the development of specific anatomic structures and morphogenetic processes, such as the development of the optic cup or the molecular and hormonal changes during fertilization and early embryogenesis (Bloch & Hew, 1960; Eakin & Brandenburger, 1967). Other stylommatophoran species whose embryogenesis has been documented include three species of giant African land snails (*Lissachatina fulica*, *Archachatina marginata* and *Limicolaria flammea*), the Roman snail (*Helix pomatia*), the grey field slug (*Deroceras agrestis*) and the leopard slug (*Limax maximus*), all of which have been described in detail based on light microscopy and illustrations (Fol, 1880; Meisenheimer, 1896; Carrick, 1939; Ghose, 1962; Egonmwan, 2007; Okon

*et al.*, 2013). However, descriptions and staging tools for stylommatophoran embryonic development using modern approaches, in tandem with high-resolution imaging, are critically missing from the literature.

Here, we characterize the embryonic development of *C. aspersum* using confocal microscopy. In tandem, we report optimized protocols for immunohistochemistry and fluorescent *in situ* hybridization in this emerging model organism. This resource is anticipated to aid future investigations of stylommatophoran developmental biology, with a focus on taxon-specific adaptations to terrestrial habitat.

## MATERIAL AND METHODS

### *Embryo cultivation and fixation*

Mature *Cornu aspersum* were housed in rectangular plastic containers (43 × 30 × 17 cm) in groups of 10–20 and kept at 22 °C. Animals were fed a mix of vegetables (e.g. sweet potato, zucchini and green leaf lettuce), calcium carbonate powder and Omega One® goldfish flakes. Each container was provided with moist coconut coir fibre substrate for egg laying. Clutches of 100–200 eggs laid in the substrate were transferred into another dish of moist coconut coir fibre and were incubated at 22 °C.

For all embryonic procedures performed on the embryos, eggs were removed from the substrate using blunt forceps and washed in reverse osmosis (RO) water. Embryos were manually removed

from the egg using sharp forceps in  $0.5 \times$  PBS or *Cepaea nemoralis* physiological solution (Bobkova *et al.*, 2004). To arrest movement in embryos in stages with retractable heads and cephalic tentacles, individuals were relaxed with menthol crystals for 30–45 min prior to fixation. Unsheathed embryos were fixed at 22 °C with either 4% paraformaldehyde or 4% formaldehyde (in  $1 \times$  PBS) for 20 min, followed by three 5-min  $1 \times$  PBST ( $1 \times$  PBS supplemented with 0.5% Tween-20) washes. Paraformaldehyde-fixed embryos were then stepwise dehydrated in ethanol, respectively, as follows: 5 min, 25% EtOH; 5 min, 50% EtOH; 5 min, 75% EtOH; three sets of 5 min 100% EtOH. Similarly, formaldehyde-fixed embryos were stepwise dehydrated in methanol. Fixed embryos were stored at  $-20$  °C in 100% EtOH or MeOH.

#### In ovo embryo cultivation

In preparation for *in ovo* cultivation, the egg was washed with RO water to ensure no substrate was present on the egg. The embryo of *C. aspersum* is surrounded by three membranes (Raven, 1966). The egg was moved into clean RO water and the tertiary (outermost) membrane on the top of the egg was removed with sharp forceps, creating a window into the egg (Supplementary Material Fig. S1). We observed that the embryo is unlikely to survive in cases where the secondary membrane (chorion) is damaged during the removal of the tertiary membrane.

To set up embryo culture, the edge of a 30-mm petri dish was lined with tissue paper dampened with RO water. Three to four windowed eggs were placed inside the 30-mm petri dish with a lid. The *in ovo* cultures were stored inside a 60-mm Petri dish lined with RO water-dampened tissue paper at room temperature in the dark. Cultures were checked regularly for contamination, embryo growth and evaporation from the tissue paper. If the cultures are not kept in a humid environment, the cultures may desiccate and fail.

#### Immunohistochemistry

Fixed embryos stored in ethanol or methanol were stepwise rehydrated into  $1 \times$  PBST over 30 min. Rehydrated embryos were incubated for 1 h in blocking solution (5% NGS, 0.1% BSA in PBST) at 22 °C. After removing the blocking solution, embryos were incubated for 20–24 h at 4 °C with a primary antibody for acetylated alpha-tubulin (T6793; Sigma-Aldrich) at 1:200 dilution in blocking solution. The primary antibody solution was removed and washed over three 5 min and three 10 min washes with PBST. Embryos were then incubated in the dark for 40–48 h at 4 °C with a secondary goat anti-mouse antibody conjugated to Alexa Fluor 594 (ThermoFisher) in a 1:200 dilution. The secondary antibody was removed by three 5 min, three 10 min and two 20 min PBST washes. During the penultimate 20 min PBST wash, embryos were incubated with Hoechst 33342 (1:2000). Embryos fixed with paraformaldehyde were incubated with phalloidin 594 conjugated to Alexa Fluor 594 (1:50) for 20 min during the final wash. Embryos were stored at 4 °C in 50% glycerol in  $1 \times$  PBS.

#### RNA extraction

Total RNA was extracted from a pool of 8-day-old embryos using TRIzol TRI Reagent (ThermoFisher), following the manufacturer's protocol. Libraries were assembled using the Illumina TruSeq library preparation kit following the manufacturer's protocol and sequenced on an Illumina NovaSeq 6000 platform with a  $2 \times 150$  bp paired end strategy at the UW-Madison BioTechnology Center, Madison, Wisconsin. Transcriptomic assembly was performed using Trinity-v2.15.0 (Grabherr *et al.*, 2011). Sequence data were deposited in GenBank under accession number PRJNA1194587.

#### Hybridization chain reaction probe design

We chose genes of interest from *Hox* and *Wnt* gene families that play a critical role during body patterning (Barucca *et al.*, 2016; Zhang *et al.*, 2024). To augment comparative expression data across Lophotrochozoa for *Hox* and *Wnt* genes, we selected the lophotrochozoan *Hox* transcription factor *Lox4* and the noncanonical *Wnt* gene *Wnt5*. To identify genes of interest for expression assays, we performed tblastn searches against the transcriptomic assembly using published peptide sequences of the transcription factors *Lox4* and *Wnt5* as queries. Query sequences consisted of the *Elysia marginata* homeobox protein *Lox4* (Genbank accession number GFR63780.1) and the *Octopus bimaculoides* protein *Wnt5* (Genbank accession number XP\_014,790,565.1). Gene identity for hits with  $e$ -value  $< 10^{-20}$  were confirmed using SMART-BLAST. After locating homologs of the two target genes in *C. aspersum*, probes for each gene of interest were designed separately using an open-source probe design platform (Kuehn *et al.*, 2022) with standard parameters, which yielded 20 probe pairs for *Lox4* and 19 probe pairs for *Wnt5*. Sequences of the probe pairs are provided in Supplementary Material Table S1.

#### In situ hybridization—hybridization chain reaction

Following a modified version of the hybridization chain reaction protocol described by Bruce *et al.* (2021), fixed embryos stored in methanol were stepwise rehydrated  $1 \times$  PBST over 30 min. Embryos were permeabilized in 500  $\mu$ l of detergent solution (1.0% SDS, 0.5% Tween, 50.0 mM Tris-HCL, 1.0 mM ethylenediaminetetraacetic acid (EDTA), 150.0 mM NaCl) at 22 °C for 30 min. After removing the detergent solution, embryos were prehybridized in 200  $\mu$ l of prewarmed probe hybridization buffer at 37 °C for 30 min. After removing the probe hybridization buffer, samples were incubated in 150  $\mu$ l of the probe solution (0.8  $\mu$ l of each probe) for 16–20 h at 37 °C. The probe solution was then removed from each sample and washed with four 15 min rinses with probe wash buffer at 37 °C. After washing out the probe solution, samples were washed twice with  $5 \times$  SSCT for 5 min at 22 °C. Embryos were then preamplified with 1 ml of pre-equilibrated amplification buffer for 30 min at 22 °C. During preamplification, 2  $\mu$ l of each hairpin (h1 and h2) corresponding to the amplifiers used for each tube were heated in 100  $\mu$ l of amplification buffer at 95 °C for 90 s, then cooled in the dark at 22 °C for 30 min. Following removal of the pre-amplification buffer, the embryos were incubated in the hairpin solution for 20–24 h at 22 °C. Hairpins were then removed by two 5 min  $5 \times$  SSCT washes, two 30 min  $5 \times$  SSCT washes, and one 5 min  $5 \times$  SSCT wash. During the last 30 min  $5 \times$  SSCT wash, the embryos were incubated with Hoechst 3342 (1:2000). Embryos were stored at 4 °C in 50% glycerol in  $1 \times$  PBS.

#### Histology

Embryos were fixed in 10% Neutral Buffered Formalin. Embedding, sectioning and staining were performed by the University of Wisconsin–Madison Histology Resource Center. For histological sectioning, embryos were embedded in paraffin and serially cross-sectioned sagittally at a thickness of 5  $\mu$ m and stained with hematoxylin and eosin (H&E) for tissue structure characterization. Deparaffinized and rehydrated sections were stained with Harris Hematoxylin for 4 min, differentiated in 1% HCl (in EtOH), then dipped in 1% ammonia (in H<sub>2</sub>O) for 30 s. Between each previous step, the sections were washed with H<sub>2</sub>O. The sections were dipped five times in 95% EtOH, then washed in eosin for 1 min. Following staining, the sections were dehydrated in 95% EtOH and cleared in xylene. The sections were covered with resinous mounting medium and a coverslip.

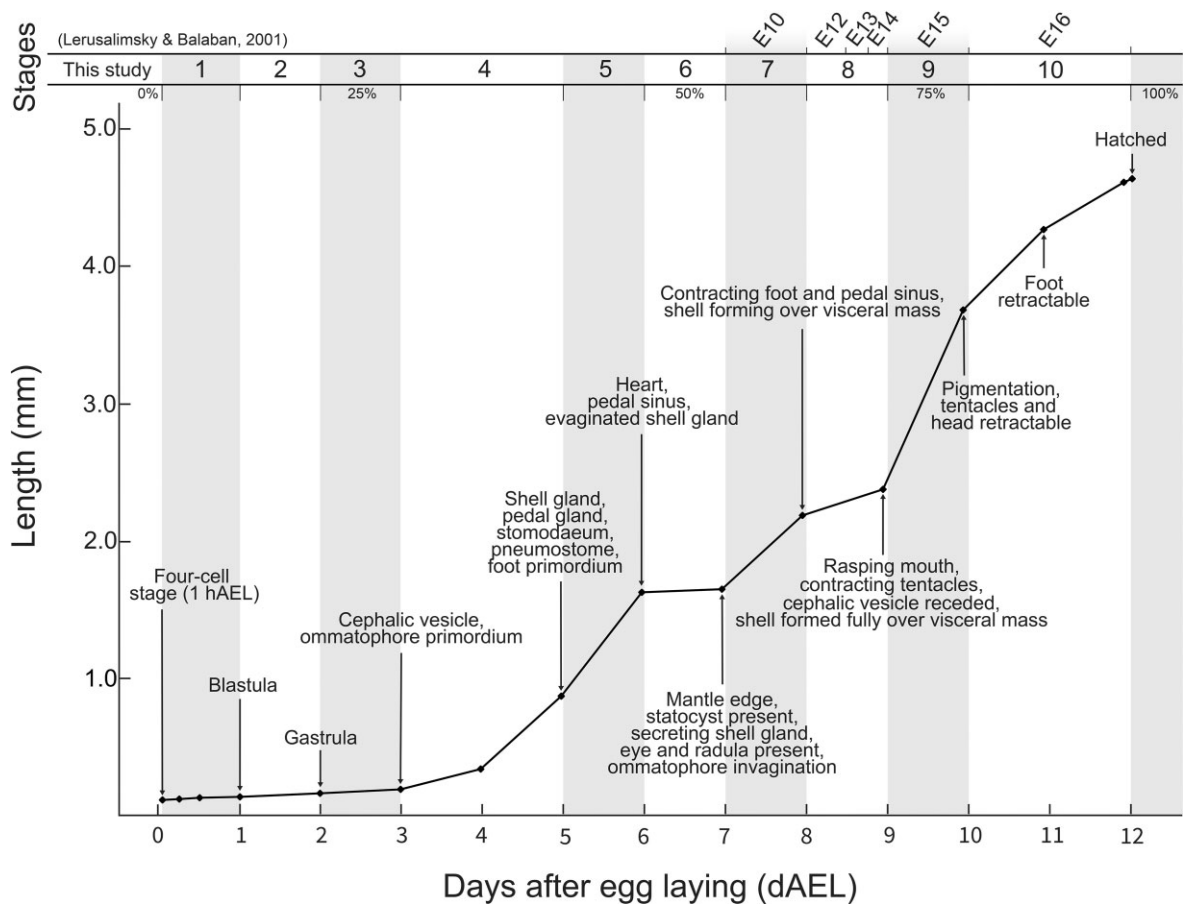


**Figure 2.** Overview of *Cornu aspersum* development and landmarks for staging system. Top: Alignment of staging systems from this study and [Jerusalimsky & Balaban \(2001\)](#).

### Mounting and imaging

Following expression assays, individual specimens were mounted in 75% glycerol in PBST or in 0.8% low melting point agarose in PBS onto glass slides. Confocal imaging was performed at the University of Wisconsin–Madison Newcomb Imaging Center using a Zeiss LSM780 and Zeiss LSM980 confocal microscope driven by Zen 2.3 SP1 (blue edition), and then processed in Zen 2.3 SP1 (blue edition) and ImageJ (Fiji 2.14.0/1.54f) with the plugin BigStitcher ([Schneider et al., 2012](#); [Hörl et al., 2019](#)). Brightfield images of whole mount embryos and H&E-stained slides were imaged on a Nikon SM225 and Olympus BX60, respectively. Figures were created in Adobe Illustrator 28.1 and Adobe Photoshop 35.3.1 (Adobe Inc., CA).

## RESULTS

### Overview of development

Mature *Cornu aspersum* individuals mate and lay egg clutches intermittently when provided continuously with fresh food and a suitable container with damp coconut fibre at 22 °C. Adult animals in the laboratory can be maintained and bred successfully throughout the year ([Fig. 1B](#)). Egg clutches are laid in shallow depressions in coconut fibre and typically contain 100–200 nearly synchronously developing embryos. Healthy eggs ([Fig. 1C, D](#)) are spherical, white in colour and measure *ca.* 5 mm in diameter. The egg has a flexible, crystalline tertiary membrane (eggshell), a thin, opaque secondary membrane (chorion) and a sticky, jelly like transparent perivitelline

fluid that consists of albumen and yolk ([Raven, 1966](#); [Tompa, 1976](#)). Upon laying, embryos require *ca.* 12 days to hatch at 22 °C ([Fig. 2](#)).

During development, *C. aspersum* gradually acquires adult features without metamorphosis or distinctive larval types. Thus, successive stages throughout the embryonic development of *C. aspersum* are defined on the basis of clearly recognizable morphological landmarks and behaviour ([Fig. 2](#)).

### *Cornu aspersum* embryos can be cultured *in ovo*

*Cornu aspersum* embryos cannot fully develop without the perivitelline fluid present within the egg. To grow embryos for the documentation of embryonic growth and behaviour, the tertiary membrane layer was manually removed ([Supplementary Material Fig. S1](#)). The embryos cultured *in ovo* may complete development in 12 days, similar to embryos growing in their original egg. However, contamination and subsequent infection of the windowed eggs may limit embryo development to 7 days, depending on infection severity.

### Stage 1–3: initial cleavages, blastula formation and early gastrulation

Stages encompassing the first cell cleavages, blastula and gastrula will be treated collectively as stages 1–3, respectively, until further study. Embryos within this range of development proved challenging to investigate in *C. aspersum* due to their susceptibility to fluctuating osmotic and oxic conditions. Attempts to manually remove the early cleavage stages from the egg without the surrounding

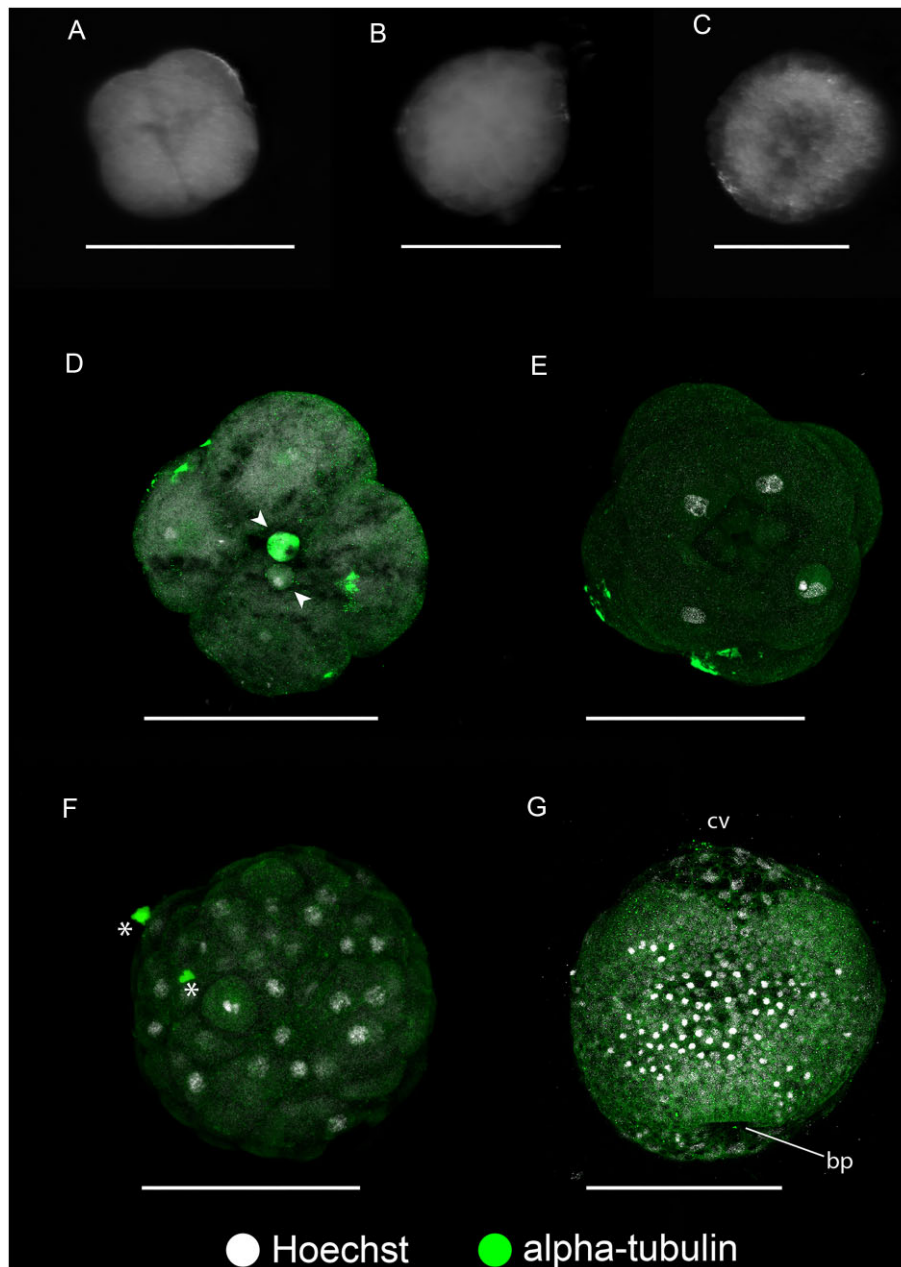


**Figure 3.** Embryonic stages 1–3 of *Cornu aspersum*. **A.** Four-cell stage embryo, corresponding to stage 1. **B.** Coeloblastula, corresponding to stage 2. **C.** Gastrula, corresponding to stage 3. **D–G.** Detail of early embryogenesis using Hoechst and immunohistochemical labeling of alpha-tubulin. **D.** Four-cell stage with visible polar bodies. **E.** Eight-cell stage. **F.** Blastula. **G.** Gastrula. Arrowhead: polar body. Asterisk: debris. Abbreviations: bp, blastopore; cv, cephalic vesicle. Scale bars: 150  $\mu\text{m}$ .

perivitelline fluid into  $0.5 \times \text{PBS}$  or *Cepaea nemoralis* physiological solution (Bobkova *et al.*, 2004) resulted in an embryo unable to form a spherical blastula or resulted in death.

Stage 1 is defined by the initial cleavages. Approximately 1 hour after egg laying, fertilized eggs contained a four-cell stage embryo with equal (= homoquadrant) dextrotropic cleavage and two polar bodies at the animal pole (Fig. 3A, D). During the third cleavage, spiral alignment of the micromeres was observed (Fig. 3E). Once the embryos had undergone multiple cellular divisions forming a coeloblastula with a wide cleavage cavity that flattens on the vegetative side, it had reached stage 2 (Fig. 3B, F). Following the formation of a spherical coeloblastula, a shallow invagination (blastopore) withdrew into the blastula until a narrow orifice (archenteron) was formed. The

appearance of the blastopore with an archenteron was indicative of stage 3, the early gastrula (Fig. 3C, G). Embryos were active at the early gastrula stage, showing translative movements within the egg.

#### Stage 4: late gastrulation and larval body formation

Following the initial formation of the archenteron, the embryo increased drastically in size and became globe-shaped (Fig. 2). Stage 4 was diagnosed by the appearance of the cephalic vesicle (= hepatic lobe, larval body and neck bladder) from the somatic plate on the dorsal side of the gastrula (Fig. 4A, B). The cephalic vesicle was bulbous and the cephalic mass cells within this area increased

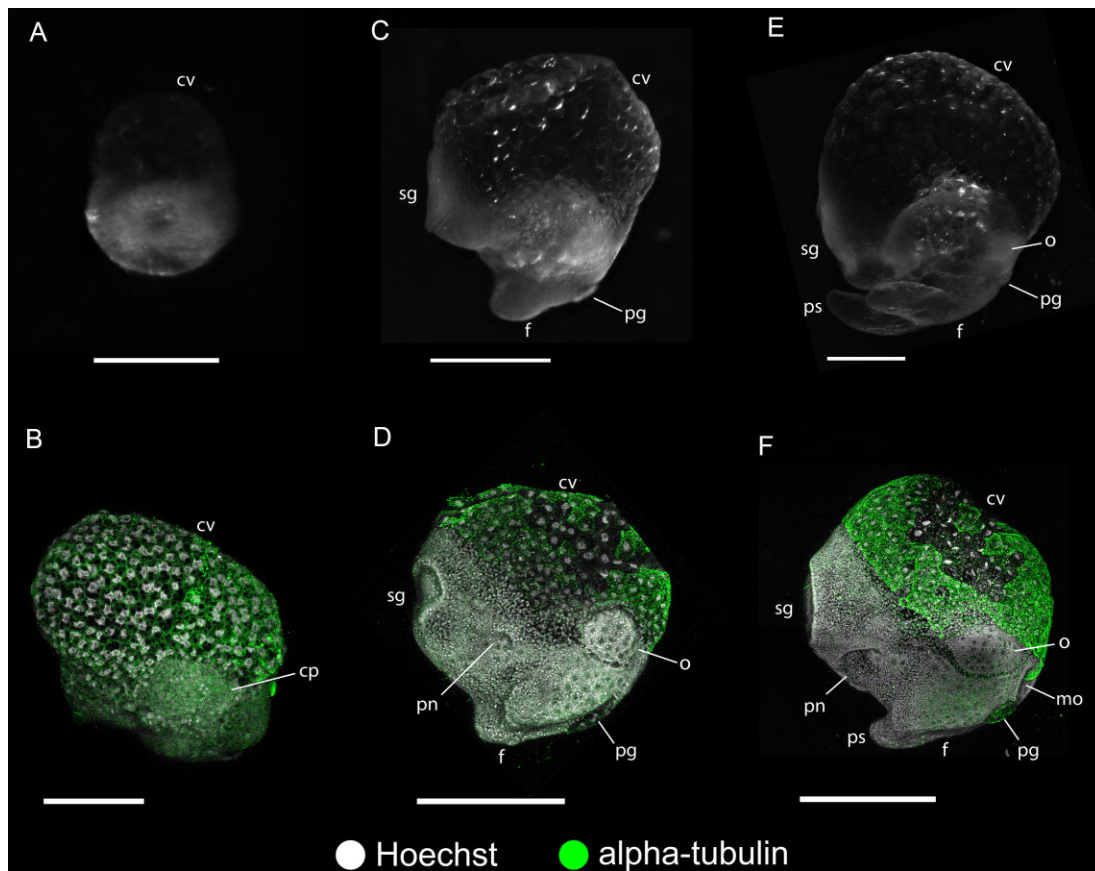


**Figure 4.** Embryonic stages 4–6 of *Cornu aspersum*. **A, B.** Stage 4 embryo in lateral view in brightfield (**A**) and Hoechst/alpha-tubulin staining (**B**). **C, D.** Stage 5 embryo in lateral view in brightfield (**C**) and Hoechst/alpha-tubulin staining (**D**). **E, F.** Stage 6 embryo in lateral view in brightfield (**E**) and Hoechst/alpha-tubulin staining (**F**). Abbreviations: cp, cephalic plate; cv, cephalic vesicle; f, foot; mo, mouth; o, ommatophore; pg, suprapedal gland; pn, pneumostome; ps, podocyst; sg, shell gland. Scale bars: **A, B**, 150  $\mu\text{m}$ ; **C–F**, 500  $\mu\text{m}$ .

considerably in size. Development of the cephalic vesicle facilitated the displacement of the blastopore to the anterior ventral side of the embryo. The posterior side of the somatic plate, opposite of the blastopore, formed the visceral hump. A thickening of ectodermal tissue on the anterior of the visceral hump formed the shell gland. The ventral plate, situated between the visceral hump and the blastopore on the ventral side of the embryo, gave rise to the foot and cephalic organs. During late gastrulation, the cephalic (sensory) plates were present as dense convex protrusions situated on the left and right anterior lateral sides of the embryo (Fig. 4B).

#### Stage 5: shell gland, foot rudiment, suprapedal gland and pneumostome rudiment

Stage 5 embryos were characterized by the appearance of the foot rudiment from the ventral plate and the shell gland as a wide invagination posterior of the somatic plate (Fig. 4C, D). Ventral to the shell gland on the right side of the visceral hump, the pneumostome primordium arose as an ectodermal invagination (Fig. 4E). The cephalic vesicle was further enlarged with hemolymph-filled cephalic mass cells, and the hemocoel of the embryo was filled with hemolymph (Supplementary Material Fig. S2). The ectoderm of the cephalic vesicle was covered with a thin membrane of strongly ciliated cells, as evident from strong alpha-tubulin expression (Fig. 4E, Supplementary Material Fig. S4A, B). Ventromedially of the cephalic vesicle, a single band of strongly vacuolated cells with long cilia was apparent on the dorsal-median of the stomodaeum (Supplementary Material Fig. S3A). The stomodaeum originated as a wide, shallow ectodermal invagination

of the anterior of the embryo above the foot rudiment and between the ommatophore primordia derived from the cephalic plates. At the anterior border of the foot (= propodium) directly ventral of the stomodaeum primordia, the suprapedal gland duct was evident as a transverse fissure with large glassy cells (Supplementary Material Fig. S3A).

#### Stage 6: podocyst, larval heart and deepening of the pneumostome

Stage 6 was marked by the presence of the podocyst (= pedal sinus, foot vesicle) developing as a dorsally bending extension of the posterior extremity of the foot (Fig. 4E, F). The podocyst is marked by epithelial cilia and microvilli. The shell gland had evaginated and extended over the surface of the dorsal surface of the visceral hump and assumed a shallow cup-like shape with an invaginated centre. The pneumostome primordium had widened and deepened into the visceral hump, in addition to being displaced posteriorly and ventrally adjacent to the edge of the shell gland (Fig. 4F). Beneath the posteroventral wall of the visceral hump near the pneumostome, the larval heart was evident and contracting strongly. On the anterior terminus of the embryo, the ommatophores increased in protuberant shape. The stomodaeum deepened, and the suprapedal gland duct opening began to narrow (Supplementary Material Fig. S3B).

#### Stage 7: torsion, eyes, shell, radula and cephalic tentacles

At stage 7, the cephalic vesicle reached its maximum size enveloping *c.* one-third of the embryo surface. The shell gland evagination

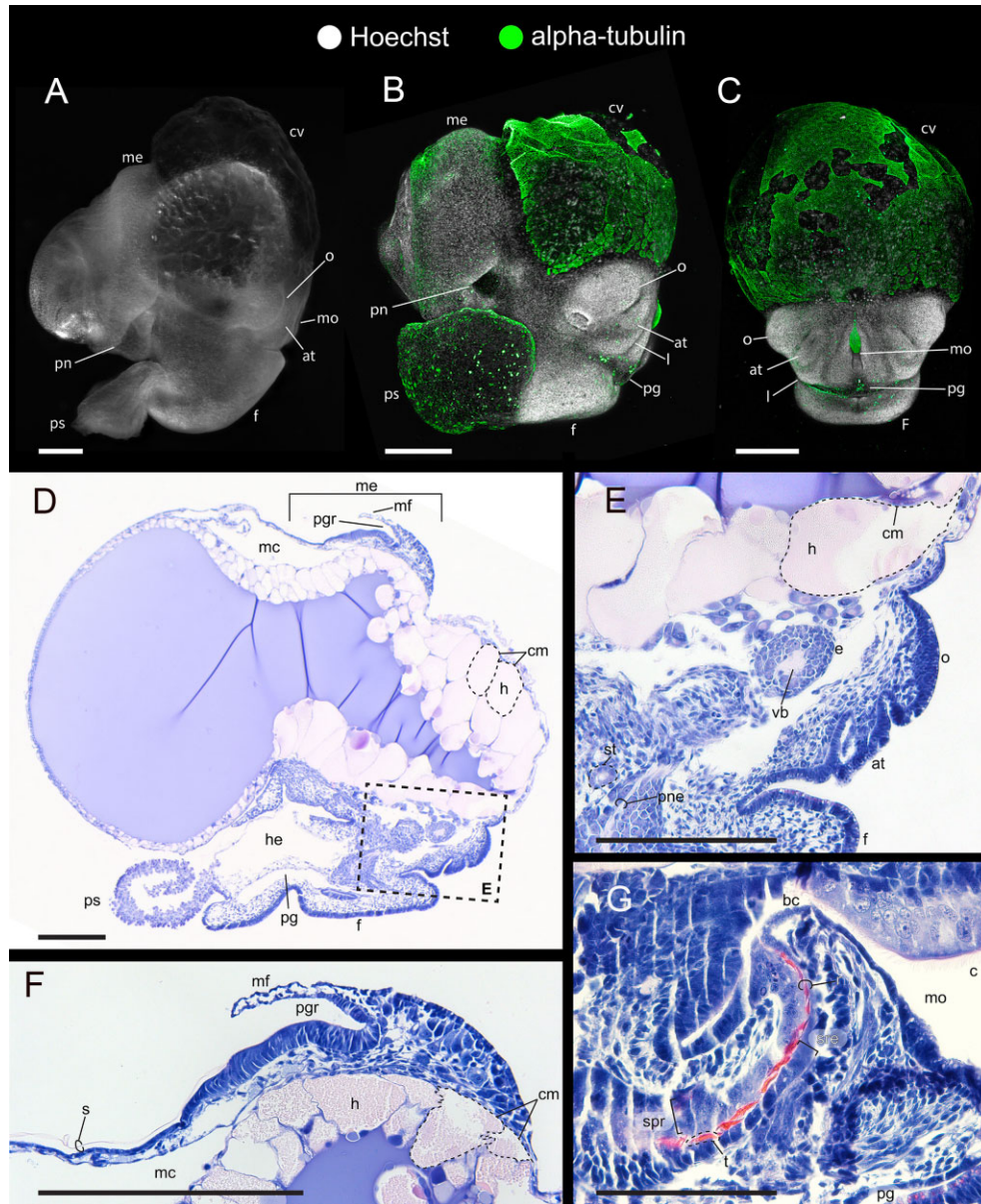


**Figure 5.** Embryonic stage 7 of *Cornu aspersum*. **A.** Brightfield imaging, in lateral view. **B.** Hoechst/alpha-tubulin staining, in lateral view. **C.** Hoechst/alpha-tubulin staining, in frontal view. **D–G.** Histological sections with hematoxylin and eosin staining. **D.** Overview of whole embryo in sagittal view. **E.** Detail of cephalic region from **D**, showing the ommatophore, anterior tentacle and developing eye. The statocyst is visible in this section. **F.** Detail of mantle fold and periostracal groove at the site of shell growth. **G.** Detail of the developing radula. Abbreviations: at, anterior tentacle; bc, buccal cavity; c, cilia; cm, cephalic mass; cv, cephalic vesicle; e, eye; f, foot; h, hemolymph; he, hemocoel; l, lip; mc, mantle cavity; me, mantle edge; mf, mantle fold; mo, mouth; o, ommatophore; pg, suprapedal gland; pgr, periostracal groove; pn, pneumostome; pne, pedal nerve; ps, podocyst; s, shell; spr, supraradular epithelium; sre, subradular epithelium; st, statocyst; vb, vitreous body. Scale bars: 250  $\mu$ m.

had progressed anteriorly over the visceral mass, which was broad, round and narrower at the posteroventral end. The anterior-most rim of the secretory margin of the shell gland had folded to form the periostracal groove (Fig. 5D, F). The periostracal groove secreted a uniformly thin layer of shell and continued to secrete the periostracum shell during the remainder of ontogeny. The pneumostome widened and expanded into the right-side of the ventral mantle edge (Fig. 5A, B). The larval heart migrated dorso-anteriorly due to torsion of the visceral mass, and its contractions were visible underneath the mantle edge.

The foot had elongated into an oblong shape and occupied the ventral surface of the embryo. The junction between the foot and the podocyst was lobate, and the podocyst had broadened with a truncate posterior edge with a sparsely ciliated epithelium (Fig. 5B). The podocyst tissue proximal to the foot was interlaced with a net-

work of anastomosing actin fibres, as evident from strong phalloidin expression (Fig. S4D, F). Both the foot and the podocyst developed contractility. The hemocoel was extended posteroventral of the foot and into the podocyst (Fig. 5D). A head-foot sulcus marked the boundary between the head and the foot. Medial to the head-foot sulcus, the suprapedal gland duct opening had diminished, and the suprapedal gland had enlarged as a tubular cavity extending posteriorly along the dorsal side of the foot (Fig. 5D). The epidermis of the suprapedal gland was composed of columnar secretory cells (Fig. 5G).

The rudiments of the anterior tentacles (= rhinophores, *sensu* Lerusalimsky & Balaban, 2001) and the lateral lips (= labial palps) were present on the antero-ventral region of the head (Fig. 5C). Proximal of the ommatophore, the eye with a vitreous body had developed from an invagination posteroventral of the ommatophore

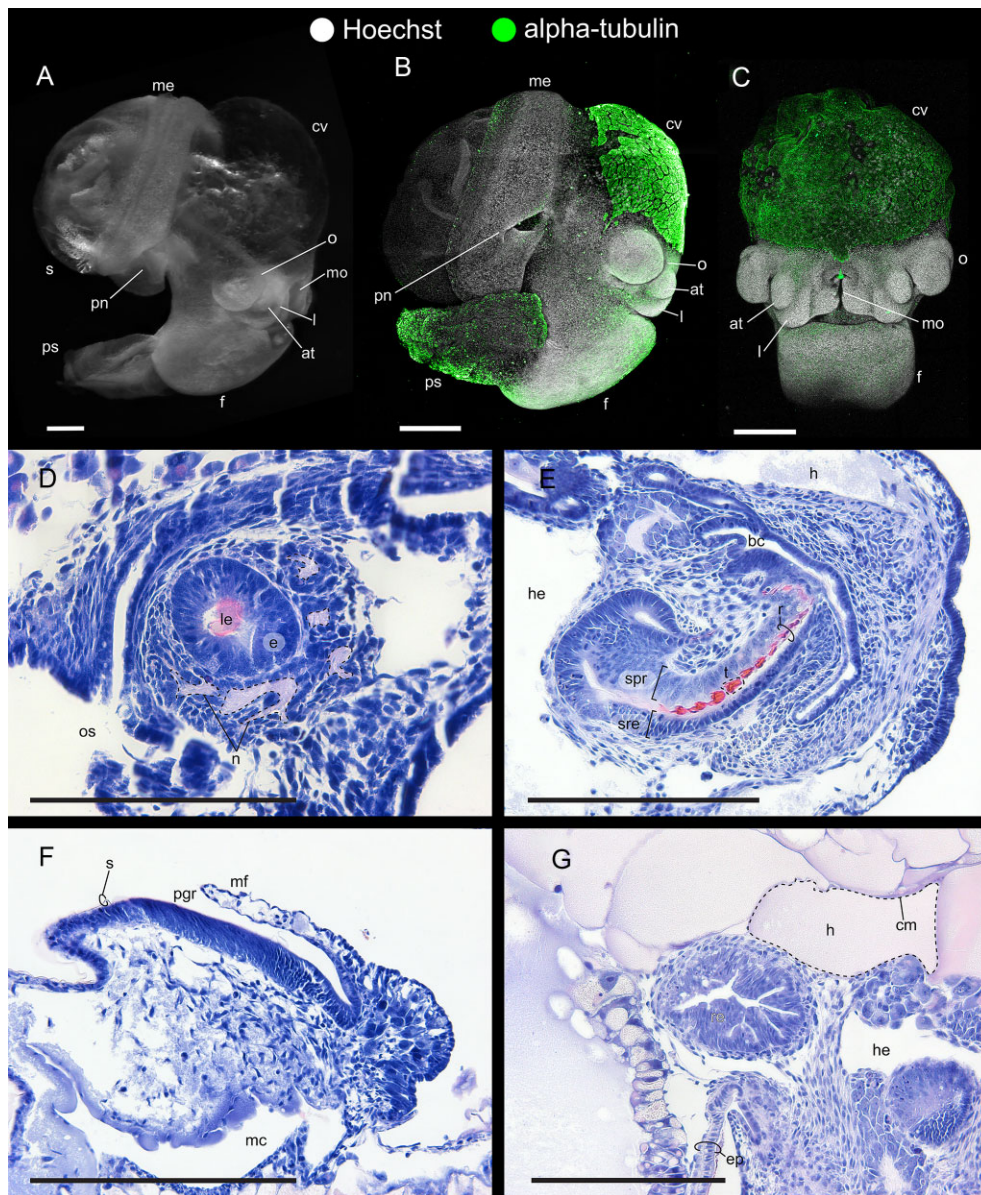


**Figure 6.** Embryonic stage 8 of *Cornu aspersum*. **A.** Brightfield imaging, in lateral view. **B.** Hoechst/alpha-tubulin staining, in lateral view. **C.** Hoechst/alpha-tubulin staining, in frontal view. **D–G.** Histological sections with hematoxylin and eosin staining. **D.** Detail of cephalic region, showing the developing eye lens. **E.** Detail of the developing radula and radular teeth. **F.** Detail of the mantle fold and periostracal groove at the site of shell growth. **G.** Detail of the hindgut. Abbreviations: at, anterior tentacle; bc, buccal cavity; cm, cephalic mass; cv, cephalic vesicle; e, eye; ep, epithelium; f, foot; h, hemolymph; he, hemocoel; l, lip; le, lens; mc, mantle cavity; me, mantle edge; mf, mantle fold; mo, mouth; n, nerve; o, ommatophore; os, outer space; pg, suprapedal gland; pgr, periostracal groove; pn, pneumostome; ps, podocyst; r, radula; re, rectum, s, shell; spr, supraradular epithelium; sre, subradular epithelium. Scale bars: 250  $\mu\text{m}$ .

(Fig. 5B, D, E) (Eakin & Brandenburger, 1967). The anterior end of the single band of ciliated cells on the dorso-medial aspect of the mouth was subulate, and the posterior end reached the buccal cavity of the mouth (Fig. 5C, G). Ventral to the mouth, the radula sac with a secreted radula had developed (Fig. 5G). The statocyst (= otolith) was present on the middorsal aspect of each lateral pedal nerve (Fig. 5E).

#### Stage 8: shell and mantle forming over visceral mass

Stage 8 was defined by the visceral mass overlain by a thin shell occupying *c.* one-third of the embryo and the cephalic vesicle beginning to reduce in size (Fig. 6A, B). Late-stage 8 embryos had a strongly reduced cephalic vesicle that resembled a fold underneath the visceral mass. The ommatophores and anterior tentacles were noticeably enlarged, and the lateral lips were well-defined

(Fig. 6B, C). There was an invagination at the distal end of the ommatophore, and the eye was innervated and had a lens (Fig. 6C, D). The row of ciliated cells on the dorso-medial region of the mouth was nearly receded into the mouth and fully receded in late-stage 8 embryos (Fig. 6C). The mouth was able to contract spontaneously, but no rasping motions were apparent. The rectum was developed and connected to the opening of the pneumostome (Fig. 6G). The posterior edge of the podocyst had divided into two lobes.

#### Stage 9: cephalic vesicle recedes, shell fully formed, contraction and rasping mouth

The cephalic vesicle was fully receded under a thinly shelled, singled-lobed mantle covering the visceral mass that resembled the

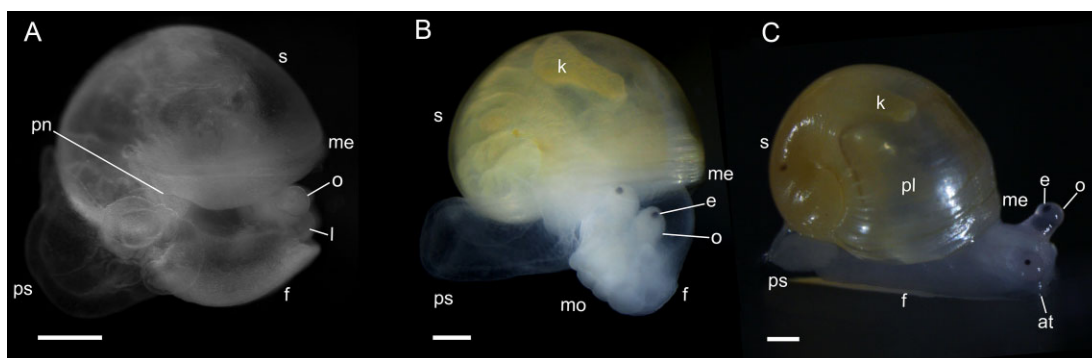


**Figure 7.** Embryonic stages 9, 10 and hatchling of *Cornu aspersum*. **A.** Stage 9 embryo in lateral view. **B.** Stage 10 embryo in lateral view. **C.** Hatchling in lateral view. Abbreviations: at, anterior tentacle; e, eye; f, foot; k, kidney; l, lip; me, mantle edge; mo, mouth; n, nerve; o, ommatophore; pl, pallial lung; pn, pneumostome; ps, podocyst; s, shell. Scale bars: 500  $\mu$ m.

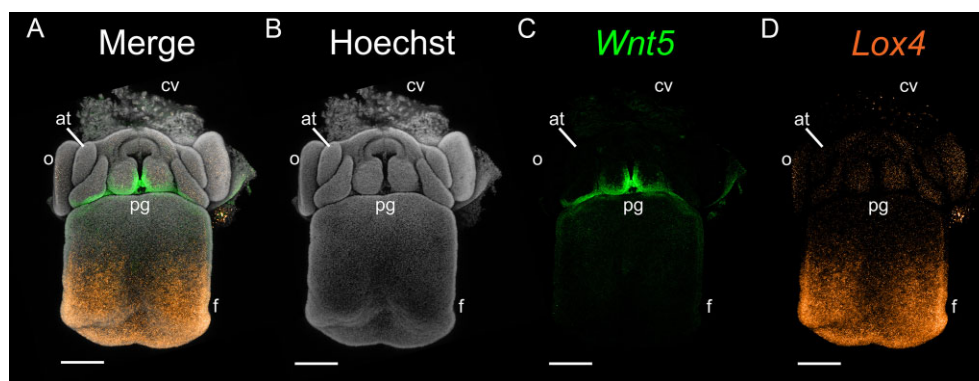


**Figure 8.** HCR gene expression assays in stage 8 embryo of *Cornu aspersum* for the genes *Wnt5* (green) and *Lox4* (orange). **A.** Merged channels. **B.** Hoechst (nuclei) layer. **C.** *Wnt5* expression. Note the concentration of transcripts in the head-foot sulcus. **D.** *Lox4* expression. Note the concentration of transcripts in the posterior foot. Abbreviations: at, anterior tentacle; cv, cephalic vesicle; f, foot; o, ommatophore; pg, suprapedal gland. Scale bars: 250  $\mu$ m.

shape of the shelled visceral mass of juvenile *C. aspersum* (Fig. 7A). The podocyst surrounded the majority of the embryo and exhibited regular, rhythmic contractions (Supplementary Material Video S1). The ommatophores and anterior tentacles were elongated and contractile (Supplementary Material Video S1). The lateral lips were enlarged but did not fully cover the mouth. The mouth was observed rasping at the perivitelline fluid (Supplementary Material Video S1). The head, but not foot, of the embryo was able to retract into the mantle cavity. The heart had migrated to the left dorsal side of the mantle cavity and was strongly beating (Supplementary Material Video S1).

#### Stage 10: retraction of body and pigmentation

At stage 10, embryos had pigmented eyespots and shells (Fig. 7B). The ommatophores and anterior tentacles were retractable into the head (Fig. 7B). All cephalic tentacles exhibited morphology comparable to postembryonic life stages. The foot was observed to contract rhythmically in retrograde monotaxic waves (Supplementary Material Video S1). The head and foot of the embryo were retractable into the mantle cavity. The kidney was visible next to the heart within the mantle cavity (Supplementary Material Video S2). At this stage, the embryos were moving frequently and continued rasping at the perivitelline fluid. Just before hatching, the embryos were rasping at the secondary and tertiary egg membranes.

#### Hatchling

Embryos at hatching were indicative of stage 11 (Fig. 7C). After the embryo ate away at the secondary and tertiary egg membranes, the

hatchling crawled out of the egg. The pallial lung emptied of fluid, and the podocyst became reduced (Fig. 7C).

#### Whole mount in situ hybridization

To demonstrate the feasibility of multiplexed *in situ* hybridization chain reaction expression assay in whole mount embryos, stage 8 was chosen due to clearly recognizable morphological landmarks during development. Expression domains resulting from the *in situ* hybridization were observed in the cephalic region and foot of the embryos (Fig. 8). The lophotrochozoan *Hox* transcription factor *Lox4*, whose expression has been previously identified to be expressed in the velum and cerebral ganglia of the vetigastropods (Samadi & Steiner, 2010), was observed to be expressed homogeneously in the cephalic vesicle, cephalic tentacles and the posteroventral side of the foot (Fig. 8D). The noncanonical *Wnt5*, known to be expressed in abalone eyes and tentacles during development (Zhang *et al.*, 2024), was restricted to the head-foot sulcus, suprapedal gland and the ventral mouth of the embryo (Fig. 8C).

## DISCUSSION

#### Differences in timing of embryonic development in *Cornu aspersum*

In *C. aspersum*, embryonic development at 22 °C spanned over a period of *ca.* 12 days. This developmental period is expectedly shorter than the embryonic development period of 16 days at 20 °C described by Ierusalimsky & Balaban (2001) and falls within the general range of 4–15 days reported between oviposition and hatching (Herzberg & Herzberg, 1962). Temperature has been shown to

influence the duration of total developmental time in marine gastropods, with an increase in developmental time corresponding to the decreases in incubation temperature (Doxa *et al.*, 2021). The variation in developmental duration of *C. aspersum* as a function of temperature accords with the generally expected effect of temperature on ontogeny in ectotherms (Pauly & Pullin, 1988; Reitzel *et al.*, 2013; Doxa *et al.*, 2021).

There are some inconsistencies in the timing of the appearance of clearly recognizable morphological landmarks during late embryogenesis. A comparison to Ierusalimsky & Balaban's (2001) description of the morphology of E10 embryos correlated to our stage 7 embryos (Fig. 2). At E10, they observed the presence of the podocyst, recognizable ommatophores and a heart on the posterior right of the visceral mass. We observed the first sign of these features earlier in development at stage 6 (Figs 2, 4E, F). Ierusalimsky & Balaban (2001) also reported that the statocyst was discernible at E12. We observed the appearance of this feature in our stage 7 embryos (Figs 2, 5E). These differences in invariant morphological development may be explained by the application of different methods used. In contrast to Ierusalimsky & Balaban (2001) who identified gamma-aminobutyric acid (GABA) immunoreactive neurons using immunocytochemistry, we stained embryos with a fluorescent nuclear dye, as well as prepared histological cross-sections for examining internal morphological landmarks, which facilitates greater clarity in the timing of morphogenesis. However, differences in staging of morphogenetic landmarks may also be attributed to thermal stress-related alterations in cell type proportions, which has been shown to incur asynchrony in developmental rate across cell types in vertebrate models (Dorrity *et al.*, 2023).

#### *Conserved patterns of cephalic vesicle growth across pulmonate gastropods*

The observations of *C. aspersum* embryonic development in the present study are consistent with the records of other stylommatophoran gastropods and comparable to descriptions of the terrestrial littorinoidean *Pomatias elegans* (Caenogastropoda) (Fol, 1880; Carrick, 1939; Creek, 1951; Ghose, 1962; Egonmwan, 2007). The large cephalic vesicle is the most prominent morphological feature present across observations of terrestrial pulmonate gastropod embryos. In the sigmurethran infraorders Achatinina, Helicina, Clausilioidei, Limacoidei and Arionoidei and the elasmognathan superfamily Succineoidea, a ciliated, contractile cephalic vesicle was observed to appear quickly after gastrulation and recede with growth of the visceral mass (Carrick, 1939; Egonmwan, 2007; Fol, 1875, 1880; Ghose, 1962; Kuchenmeister, 1996; Schmidt, 1895). In *C. aspersum*, we observed the cephalic vesicle comprised of substantial cephalic mass cells containing hemolymph and large vacuoles filled with albumen to appear after gastrulation (stage 4) and was present until the structure receded (stage 9). It has been suggested that the cephalic vesicle of stylommatophorans represents a velum modified to facilitate the circulation of hemolymph throughout the embryo through contractions (Fol, 1880; Schmidt, 1895). While further investigations using genetic approaches (i.e. gene sequencing, expression, functional manipulations) are necessary to confirm the homology between the cephalic vesicle and the velum, we observed the cephalic vesicle to contract, which is in accordance with facilitating the movement of hemolymph throughout the hemocoel.

A superficially similar structure is present after gastrulation in the terrestrial littorinoidean *P. elegans* (Creek, 1951). Creek (1951) described a cephalic mass comprised of large vacuolated epithelial cells bearing short cilia to facilitate the movement of albumen into the embryo rather than acting as a contractile vesicle that circulates hemolymph throughout the hemocoel of the embryo. He suggested that the only difference between the cephalic mass of *P. elegans* and the velar tissue of the periwinkle *Littorina obtusata littoralis* is the presence of large vacuolated cells filled with albumen of the second

layer of the epithelium. This uptake and absorption of albumen coincides with the observations in this study and the descriptions of the stylommatophorans *Lissachatina fulica* and *Lissachatina agrestis*, wherein albumen is taken up into the early cephalic vesicle before transport into the hepatic lobe and larval gut (Carrick, 1939; Ghose, 1962).

The hypertrophy of the cephalic region is not limited to completely terrestrial gastropod taxa; some semiaquatic or semiterrestrial species that develop in terrestrial environments and select marine gastropods exhibit an enlargement of the cephalic region, albeit to a lesser extent than terrestrial pulmonates (Demain & Yousif, 1973; Meshcheryakov, 1990; Ranjah, 1942). Embryonic development of the aquatic pulmonate Ampullariidae (Caenogastropoda) and *Lymnaea stagnalis* (Heterobranchia) encompasses a cephalic vesicle-like structure that recedes after the visceral mass progresses anteriorly (Accorsi *et al.*, 2024; Demain & Yousif, 1973; Koch *et al.*, 2009; Meshcheryakov, 1990; Ranjah, 1942). Outside of pulmonate gastropods, Collin (2000) has documented a densely ciliated translucent head vesicle on the head of the littorinoidean *Crepipatella linguata* during development. The cephalic vesicle-like structures of each described development do not reach the profound size of that found in Stylommatophora or *P. elegans*, but the structure is comprised of an ectodermal layer of large vacuolated cells with inner space is similar in function as a larval stomach filled with albumen (Demain & Yousif, 1973; Koch *et al.*, 2009; Ranjah, 1942).

While the cephalic vesicle can be found in multiple lineages of gastropod embryos during development, the structure is the most protuberant in terrestrial pulmonated gastropods. The large vacuolated epithelial cells of the cephalic vesicle suggest a function of undertaking nutrients from the egg capsule fluid, and the mass enlargement of the vesicle within stylommatophorans and terrestrial littorinoideans may be attributed to the precociously developed larval gut and the little yolk content found in the perivitelline fluid of the egg capsules common in terrestrial gastropods (Carrick, 1939; Creek, 1951; Fol, 1880). Further growth of the cephalic vesicle within stylommatophorans may be exacerbated by the need to circulate hemolymph throughout the embryo before the appearance of the beating larval heart (Fol, 1880). Our observation of a contractile cephalic vesicle with hemolymph cavities and large vacuoles filled with albumen, supports the suggested function of facilitating hemolymph circulation and absorption of albumen.

#### *The podocyst within Stylommatophora*

The podocyst (= pedal sinus) is a large, thin transparent sac covered extensively with ciliated microvilli attached to the posterior of the foot only observed in oviparous sigmurethran embryos (Schmidt, 1895; Cather & Tompa, 1972; Kuchenmeister, 1996; Ierusalimsky & Balaban, 2001). The podocyst functions primarily as a pseudo-larval heart that contracts and relaxes rhythmically to maintain the circulation of hemocoel in conjunction with the cephalic vesicle (Carrick, 1939; Ghose, 1962; Kuchenmeister, 1996). In *Deroceras agrestis*, the podocyst and cephalic vesicle arise and antiphasically pulsate (cephalo-pedal pumping) prior to onset of heart activity, and, after inception of heart pulsation, the frequency of oscillating contractions lower with the growth of the embryo (Kuchenmeister, 1996). Cather & Tompa (1972) have demonstrated that the podocyst has a secondary albumentrophic and calcium resorption function due to the ultrastructural microvilli on the external surface. In *C. aspersum*, we observed a cilia- and microvilli-covered podocyst begin to develop at stage 6 (Fig. 4E, Supplementary Material Fig. S4D, F). At this stage, the heart was actively beating in conjunction with the appearance of the podocyst (Fig. 2).

Surprisingly, Succineoidea (Elasmognatha) has been observed to not develop a podocyst or vestige of the podocyst despite the presence of a cephalic vesicle and yolk-poor perivitelline fluid similar to oviparous sigmurethans (Cather & Tompa, 1972;

Schmidt, 1895). The placement of Elasmognatha within Eupulmonata has remained contentious; previous proposals built on morphological data such as the embryonic kidney, lack of podocyst, uncalcified egg and cerebral ganglia suggested Elasmognatha to be more closely related to Basommatophora than to Sigmurethra and Orthurethra (Cather & Tompa, 1972; Tompa, 1984). More recent analyses using mitogenomic data have suggested Elasmognatha to reside within Sigmurethra as the sister group of Helicoidea + Urocoptoidea with Arionoidea falling outside this clade (Doğan *et al.*, 2020; Guzmán *et al.*, 2021). Although morphological evidence alone is inadequate to resolve the taxonomic position of Elasmognatha relative to Stylommatophora, more detailed documentation of stylommatophoran embryonic development may reveal evolutionary trends of these groups by complementing genetic data.

## CONCLUSION

Terrestrial gastropods remain underrepresented in modern evolutionary developmental investigations of major evolutionary transitions within Gastropoda. Stylommatophora exhibit numerous anatomical innovations and genome duplication, potentially making this group useful in the study of macroevolutionary phenomena (Liu *et al.*, 2021; Chen *et al.*, 2022). Some stylommatophorans also exhibit unique behaviours, such as production of epiphragms during aestivation and complex courtship behaviours (Barker, 2001; Shimizu *et al.*, 2019). Here, we developed an embryonic staging system and protocols for the study of *C. aspersum* development, with the aim of equipping renewed investigations of stylommatophoran biology. Together with the availability of embryonic transcriptomic data and a chromosomal-level genome assembly (GenBank accession number PRJEB76641; Parmakelis *et al.*, 2017), we anticipate that *C. aspersum* will serve as a useful platform for understanding the mechanistic basis for gastropod terrestrialization and testing the impact of whole genome duplication on stylommatophoran diversification dynamics.

## SUPPLEMENTARY MATERIAL

Supplementary material is available at *Journal of Molluscan Studies* online.

## ACKNOWLEDGEMENTS

Imaging was performed at the Newcomb Imaging Center (NIC), Department of Botany, University of Wisconsin-Madison, with the help of Sarah Swanson. Benjamin C. Klementz, Emily V.W. Setton, Sophie M. Neu and Ethan M. Laumer assisted with the care and maintenance of *C. aspersum*. Histological embedding, sectioning and staining was performed by the University of Wisconsin-Madison Histology Resource Center (HRC).

## FUNDING

This work was supported by the National Science Foundation grant no. IOS-2016141 to PPS, as well as the 2023 Dee Saunders Dundee Memorial Research Grant (Malacology Research Award) to K.M.A. The funders had no role in study design, data collection and analysis, publication or manuscript preparation.

## CONFLICT OF INTEREST

The authors have no conflicts of interest to declare.

## REFERENCES

- ACCORSI, A., PARDO, B., ROSS, E., CORBIN, T.J., MCCLAIN, M., WEAVER, K., DELVENTHAL, K., MORRISON, J.A., MCKINNEY, M.C., MCKINNEY, S.A. & ALVARADO, A.S. 2024. A new genetically tractable non-vertebrate system to study complete camera-type eye regeneration. *BioRxiv*. Available at: <https://doi.org/10.1101/2024.01.26.577494> (24 October 2024, date last accessed).
- BARKER, G.M. (Ed.), 2001. *The biology of terrestrial molluscs*. CABI Publishing, Wallingford, UK.
- BARUCCA, M., CANAPA, A. & BISCOTTI, M.A. 2016. An overview of *Hox* genes in Lophotrochozoa: evolution and functionality. *Journal of Developmental Biology*, **4**: 12.
- BIELER, R. 1992. Gastropod phylogeny and systematics. *Annual Review of Ecology and Systematics*, **23**: 311–338.
- BLOCH, D.P. & HEW, H.Y.C. 1960. Changes in nuclear histones during fertilization, and early embryonic development in the pulmonate snail, *Helix aspersa*. *The Journal of Cell Biology*, **8**: 69–81.
- BOBKOVA, M.V., GÁL, J., ZHUKOV, V.V., SHEPELEVA, I.P. & MEYER-ROCHOW, V.B. 2004. Variations in the retinal designs of pulmonate snails (Mollusca, Gastropoda): squaring phylogenetic background and ecophysiological needs (I). *Invertebrate Biology*, **123**: 101–115.
- BRENZINGER, B., SCHRÖDL, M. & KANO, Y. 2021. Origin and significance of two pairs of head tentacles in the radiation of euthyneuran sea slugs and land snails. *Scientific Reports*, **11**: 21016.
- BROWN, K.M. & LYDEARD, C. 2010. Mollusca: Gastropoda. In: *Ecology and classification of North American freshwater invertebrates*, Edn 3 (J. H. THORP & A. P. COVICH, eds), pp. 277–306. Academic Press, San Diego, CA.
- BRUCE, H.S., JERZ, G., KELLY, S., MCCARTHY, J., POMERANTZ, A., SENEVIRATHNE, G., SHERRARD, A., SUN, D.A., WOLFF, C. & PATEL, N.H., 2021. Hybridization chain reaction (HCR) in situ protocol. protocols.io.
- BURCH, J.B. 1962. *How to know the eastern land snails: pictured-keys for determining the land snails of the United States occurring east of the Rocky Mountain Divide*. W.C. Brown Company, Dubuque, IA.
- CARRICK, R. 1939. The life-history and development of *Agriolimax agrestis* L., the gray field slug. *Transactions of the Royal Society of Edinburgh*, **59**: 563–597.
- CATHER, J. & TOMPA, A. 1972. The podocyst in pulmonate evolution. *Malacological Review*, **5**: 1–3.
- CHEN, Z., DOĞAN, Ö., GUIGLIELMONI, N., GUICHARD, A. & SCHRÖDL, M. 2022. Pulmonate slug evolution is reflected in the *de novo* genome of *Arion vulgaris* Moquin-Tandon, 1855. *Scientific Reports*, **12**: 14226.
- CLEMENT, A.C. 1962. Development of *Ilyanassa* following removal of the D macromere at successive cleavage stages. *Journal of Experimental Zoology*, **149**: 193–215.
- COLLIN, R. 2000. Sex change, reproduction, and development of *Crepidula adunca* and *Crepidula lingulata* (Gastropoda: Calyptraeidae). *The Velliger*, **43**: 24–33.
- CONKLIN, E.G. 1897. The embryology of *Crepidula*, a contribution to the cell lineage and early development of some marine gastropods. *Journal of Morphology*, **13**: 1–226.
- CREEK, G.A. 1951. The reproductive system and embryology of the snail *Pomatias elegans* (Müller). *Proceedings of the Zoological Society of London*, **121**: 599–640.
- DAYRAT, B. & TILLIER, S. 2002. Evolutionary relationships of euthyneuran gastropods (Mollusca): a cladistic re-evaluation of morphological characters. *Zoological Journal of the Linnean Society*, **135**: 403–470.
- DEMAIN, E.S. & YOUSIF, F.O.U.A.D. 1973. Embryonic development and organogenesis in the snail *Marisa cornuarietis* (Mesogastropoda: Ampullariidae)—IV: development of the shell gland, mantle and respiratory organs. *Malacologia*, **12**: 195–211.
- DOĞAN, Ö., SCHRÖDL, M. & CHEN, Z. 2020. The complete mitogenome of *Arion vulgaris* Moquin-Tandon, 1855 (Gastropoda: Stylommatophora): mitochondrial genome architecture, evolution and phylogenetic considerations within Stylommatophora. *PeerJ*, **8**: e8603.
- DORRITY, M.W., SAUNDERS, L.M., DURAN, M., SRIVATSAN, S.R., BARKAN, E., JACKSON, D.L., SATTLER, S.M., EWING, B.,

- QUEITSCH, C., SHENDURE, J., RAIBLE, D.W., KIMELMAN, D. & TRAPNELL, C. 2023. Proteostasis governs differential temperature sensitivity across embryonic cell types. *Cell*, **186**: 5015–5027.e12.
- DOXA, C.K., STERIOTI, A., DIVANACH, P. & KENTOURI, M. 2021. Effect of temperature on embryonic development of the marine gastropod *Charonia sequegnae* (Aradas & Benoit, 1870). *Journal of Thermal Biology*, **100**: 103044.
- EAKIN, R.M. & BRANDENBURGER, J.L. 1967. Differentiation in the eye of a pulmonate snail *Helix aspersa*. *Journal of Ultrastructure Research*, **18**: 391–421.
- EGONMWAN, R.I. 2007. Light and electron microscopy study of late embryonic development in the land snail *Limicolaria flammea* (Müller) (Pulmonata, Achatinidae). *Revista Brasileira de Zoologia*, **24**: 436–441.
- FOL, H. 1875. Études sur le développement des mollusques. Sur le développement des ptéropodes. Première mémoire. Archives de zoologie expérimentale et générale, Tome 4. Centre National de la Recherche Scientifique, Paris.
- FOL, H. 1880. Études sur le développement des mollusques. Archives de zoologie expérimentale et générale, **8**: 103–232.
- GEORGESCU, M., DRĂGHICI, G.A., OANCEA, E.-F., DEHELEAN, C.A., ȘOICA, C., VLĂDUȚ, N.-V. & NICA, D.V. 2021. Effects of cadmium sulfate on the brown garden snail *Cornu aspersum*: implications for DNA methylation. *Toxics*, **9**: 306.
- GHOSE, K.C. 1962. Embryogenesis and larval organs of the giant land snail *Achatina fulica* Bowdich. *Proceedings of the Royal Society of Edinburgh. Section B. Biology*, **68**: 237–260.
- GOODHEART, J.A., RIO, R.A., TARAPOREVALA, N.F., FIORENZA, R.A., BARNES, S.R., MORRILL, K., JACOB, M.A.C., WHITESEL, C., MASTERSON, P., BATZEL, G.O., JOHNSTON, H.T., RAMIREZ, D., KATZ, P.S. & LYONS, D.C. 2024. A chromosome-level genome for the nudibranch gastropod *Berghia stephanieae* helps parse clade-specific gene expression in novel and conserved phenotypes. *BMC Biology*, **22**: 9.
- GRABHERR, M.G., HAAS, B.J., YASSOUR, M., LEVIN, J.Z., THOMPSON, D.A., AMIT, I., ADICONIS, X., FAN, L., RAYCHOWDHURY, R., ZENG, Q., CHEN, Z., MAUCELI, E., HACOEN, N., GNIIRKE, A., RHIND, N., PALMA, F.D., BIRREN, B.W., NUSBAUM, C., LINDBLAD-TOH, K., FRIDEMAN, N. & REGEV, A. 2011. Full-length transcriptome assembly from RNA-Seq data without a reference genome. *Nature Biotechnology*, **29**: 644.
- GRANDE, C. & PATEL, N.H. 2009. Nodal signalling is involved in left-right asymmetry in snails. *Nature*, **457**: 1007.
- GULLER, A. & MADEC, L. 2010. Historical biogeography of the land snail *Cornu aspersum*: a new scenario inferred from haplotype distribution in the Western Mediterranean basin. *BMC Evolutionary Biology*, **10**: 18.
- GUZMÁN, L.B., VOGLER, R.E. & BELTRAMINO, A.A. 2021. The mitochondrial genome of the semi-slug *Omalonyx unguis* (Gastropoda: Succineidae) and the phylogenetic relationships within Stylommatophora. *PLoS One*, **16**: e0253724.
- HASZPRUNAR, G. & WANNINGER, A. 2012. Molluscs. *Current Biology*, **22**: R510–R514.
- HERZBERG, F. & HERZBERG, A. 1962. Observations on reproduction in *Helix aspersa*. *American Midland Naturalist*, **68**: 297.
- HÖRL, D., ROJAS RUSAK, F., PREUSSER, F., TILLBERG, P., RANDEL, N., CHHETRI, R.K., CARDONA, A., KELLER, P.J., HARZ, H., LEONHARDT, H., TREIER, M. & PREIBISCH, S. 2019. BigStitcher: reconstructing high-resolution image datasets of cleared and expanded samples. *Nature Methods*, **16**: 870–874.
- IERUSALIMSKY, V.N. & BALABAN, P.M. 2001. Ontogenesis of the snail, *Helix aspersa*: embryogenesis timetable and ontogenesis of GABA-like immunoreactive neurons in the central nervous system. *Journal of Neurocytology*, **30**: 73–91.
- ITZIOU, A., PATSIS, P.A. & DIMITRIADIS, V.K. 2018. Introduction of the land snail *Cornu aspersum* as a bioindicator organism of terrestrial pollution with the use of a suite of biomarkers. *Toxicological & Environmental Chemistry*, **100**: 717–736.
- KNIGHT, M., MILLER, A., LIU, Y., SCARIA, P., WOODLE, M. & ITIPRASERT, W. 2011. Polyethyleneimine (PEI) Mediated siRNA Gene Silencing in the *Schistosoma mansoni* Snail Host, *Biomphalaria glabrata*. *PLoS Neglected Tropical Diseases*, **5**: e1212.
- KOCH, E., WINIK, B.C. & CASTRO-VAZQUEZ, A. 2009. Development beyond the gastrula stage and digestive organogenesis in the apple-snail *Pomacea canaliculata* (Architaenioglossa, Ampullariidae). *Biocell*, **33**: 49–65.
- KUCHENMEISTER, G.M. 1996. Quantification of the development of the cephalic sac and podocyst in the terrestrial gastropod *Limax maximus* L. *Malacologia*, **38**: 153–160.
- KUEHN, E., CLAUSEN, D.S., NULL, R.W., METZGER, B.M., WILLIS, A.D. & ÖZPOLAT, B.D. 2022. Segment number threshold determines juvenile onset of germline cluster expansion in *Platynereis dumerilii*. *Journal of Experimental Zoology Part B: Molecular and Developmental Evolution*, **338**: 225–240.
- KURODA, R. & ABE, M. 2020. The pond snail *Lymnaea stagnalis*. *EvoDevo*, **11**: 24.
- LESOWAY, M.P. & HENRY, J.Q. 2019. Twisted shells, spiral cells, and asymmetries: evo-devo lessons learned from gastropods. In: *Evolutionary developmental biology: a reference guide* (L. NUNO DE LA ROSA & G. MÜLLER, eds.), pp. 1–18. Springer, Cham.
- LIU, C., REN, Y., LI, Z., HU, Q., YIN, L., WANG, H., QIAO, X., ZHANG, Y., XING, L., XI, Y., JIANG, F., WANG, S., HUANG, C., LIU, B., LIU, H., WAN, F., QIAN, W. & FAN, W. 2021. Giant African snail genomes provide insights into molluscan whole-genome duplication and aquatic–terrestrial transition. *Molecular Ecology Resources*, **21**: 478–494.
- LYONS, D.C., PERRY, K.J. & HENRY, J.Q. 2015. Spiralian gastrulation: germ layer formation, morphogenesis, and fate of the blastopore in the slipper snail *Crepidula fornicata*. *EvoDevo*, **6**: 24.
- LYONS, D.C., PERRY, K.J., LESOWAY, M.P. & HENRY, J.Q. 2012. Cleavage pattern and fate map of the mesentoblast, 4d, in the gastropod *Crepidula*: a hallmark of spiralian development. *EvoDevo*, **3**: 21.
- MADEC, L., DESBUQUOIS, C. & COUTELLEC-VRETO, M.-A. 2000. Phenotypic plasticity in reproductive traits: importance in the life history of *Helix aspersa* (Mollusca: Helicidae) in a recently colonized habitat. *Biological Journal of the Linnean Society*, **69**: 25–39.
- MCDERMOTT, M., CERULLO, A.R., PARZIALE, J., ACHRAK, E., SULTANA, S., FERD, J., SAMAD, S., DENG, W., BRAUN-SCHWEIG, A.B. & HOLFORD, M. 2021. Advancing discovery of snail mucins function and application. *Frontiers in Bioengineering and Biotechnology*, **9**: 734023.
- MEISENHEIMER, v.J. 1896. Entwicklungsgeschichte von *Limax maximus* L. II Theil. Die Larvenperiode. *Zeitschrift für Wissenschaftliche Zoologie*, **63**: 573–664.
- MESHCHERYAKOV, V.N. 1990. *The common pond snail Lymnaea stagnalis*. In: *Animal species for developmental studies. Vol. 1. Invertebrates* (T. A. DETTLAFF & S. G. VASSETZKY, eds), pp. 69–132. Consultants Bureau, New York.
- MORDAN, P. & WADE, C. 2008. Heterobranchia II: the Pulmonata. In: *Phylogeny and evolution of the Mollusca* (W. PONDER & D.R. LINDBERG, eds), pp. 409–426. University of California Press, Berkeley, CA.
- OKON, B., IBOM, L.A., EBENSO, I.E. & BASSEY, A.E. 2013. Developmental stages and quality traits of giant African land snails [*Archachatina marginata* (Swainson)] eggs. *Natural Science*, **05**: 1121–1126.
- PARMAKELIS, A., KOTSAKIOZI, P., KONTOS, C.K., ADAMOPOULOS, P.G. & SCORILAS, A. 2017. The transcriptome of a “sleeping” invader: *de novo* assembly and annotation of the transcriptome of aestivating *Cornu aspersum*. *BMC Genomics*, **18**: 491.
- PAULY, D. & PULLIN, R.S.V. 1988. Hatching time in spherical, pelagic, marine fish eggs in response to temperature and egg size. *Environmental Biology of Fishes*, **22**: 261–271.
- PERRY, K.J. & HENRY, J.Q. 2015. CRISPR/Cas9-mediated genome modification in the mollusc, *Crepidula fornicata*. *Genesis*, **53**: 237–244.
- RANJAH, A.R. 1942. The embryology of the Indian apple-snail, *Pila globosa* (Swainson) [Mollusca, Gastropoda]. *Records of the Indian Museum*, **44**: 217–322.
- RAVEN, P. 1966. *Oogenesis*. In: *Morphogenesis* (P. RAVEN, ed.), pp. 1–21. Pergamon Press, Oxford, UK.
- REITZEL, A., CHU, T., EDQUIST, S., GENOVESE, C., CHURCH, C., TARRANT, A. & FINNERTY, J. 2013. Physiological and developmen-

- tal responses to temperature by the sea anemone *Nematostella vectensis*. *Marine Ecology Progress Series*, **484**: 115–130.
- ROSENBERG, G. 2014. A new critical estimate of named species-level diversity of the Recent Mollusca. *American Malacological Bulletin*, **32**: 308–322.
- RUTHENSTEINER, B. 1997. Homology of the pallial lung and pulmonary cavity of gastropods. *Journal of Molluscan Studies*, **63**: 353–367.
- SAMADI, L. & STEINER, G. 2010. Expression of Hox genes during the larval development of the snail, *Gibbula varia* (L.)—further evidence of non-colinearity in molluscs. *Development Genes and Evolution*, **220**: 161–172.
- SCHMIDT, F. 1895. Beiträge der Entwicklungsgeschichte der Stylommatophoren. *Zoologische Jahrbucher, Abteilung Für Anatomie Und Ontogenie Der Thiere*, **8**: 318–341.
- SCHNEIDER, C.A., RASBAND, W.S. & ELICEIRI, K.W. 2012. NIH ImageJ: 25 years of image analysis. *Nature Methods*, **9**: 671–675.
- SHIMIZU, K., KIMURA, K., ISOWA, Y., OSHIMA, K., ISHIKAWA, M., KAGI, H., KITO, K., HATTORI, M., CHIBA, S. & ENDO, K. 2019. Insights into the evolution of shells and love darts of land snails revealed from their matrix proteins. *Genome Biology and Evolution*, **11**: 380–397.
- SMITH, A.M. 2010. Gastropod secretory glands and adhesive gels. In: *Biological Adhesive Systems* (J. VON BYERN & I. GRUNWALD, eds), pp. 41–51. Springer, Vienna.
- TOMPA, A.S. 1976. A comparative study of the ultrastructure and mineralogy of calcified land snail eggs (Pulmonata: Stylommatophora). *Journal of Morphology*, **150**: 861–887.
- TOMPA, A.S. 1984. Land snails (Stylommatophora). In: *Reproduction* (K.M. WILBUR, N.H. VERDONK, A.S. TOMPA & J.A.M. VAN DEN BIGGELAAR, eds), pp. 47–140. Academic Press, Orlando, FL.
- YANG, Z., ZHANG, L., HU, J., WANG, J., BAO, Z. & WANG, S. 2020. The evo-devo of molluscs: Insights from a genomic perspective. *Evolution & Development*, **22**: e12336.
- ZHANG, Q., FU, Y., ZHANG, Y. & LIU, H. 2024. Genome-wide identification and expression profiling of the Wnt gene family in three abalone species. *Genes & Genomics*, **46**: 1363–1374.